NANO LETTERS

2007
Vol. 7, No. 8
2417−2421

Synthesis of Uniform Double-Walled Carbon Nanotubes Using Iron Disilicide as Catalyst

Hang Qi, Cheng Qian, and Jie Liu*

Department of Chemistry, Duke University, Durham, North Carolina 27708

Received May 9, 2007; Revised Manuscript Received June 19, 2007

ABSTRACT

The preparation of carbon nanotube (CNT) materials with high purity is critical for many potential applications. These materials not only need to be free of carbonaceous impurities but also have uniform diameters. Within the CNT family, double-walled carbon nanotubes (DWNTs), as the simplest member of multiwalled carbon nanotubes, have demonstrated good potential in many bulk applications. However, the synthesis of DWNTs with uniform diameter and high purity is still a challenge. Here, a method to prepare high-purity DWNTs using iron disilicide ($FeSi_2$) as catalyst is demonstrated. Over 90% of CNTs in the sample were DWNTs with a narrow diameter distribution in the range of 4–5 nm. An additional advantage of using $FeSi_2$ as catalyst is to simplify the process to prepare suitable catalyst because commercially available $FeSi_2$ can be used directly without any further treatment.

Carbon nanotubes (CNT) is a family of materials that possesses appealing properties for many potential applications. However, the preparation of CNT samples with high purity is still a challenge. The words "high purity" here have two meanings. One is that the materials are free of carbonaceous species other than CNTs and the other is that the sample only consists of CNTs with the same number of walls and/or diameter. The diameter of CNT is an important parameter, for it not only determines the energy gap of the semiconducting CNTs[1−3] but also modulates the interaction between CNTs and adsorbed molecules such as H_2.[4] Earlier experiments have demonstrated that preparing identical catalyst particles is an effective way to obtain uniform CNT samples using chemical vapor deposition method (CVD).[5] The diameters of CNTs are known to be proportionally related to the sizes of the catalyst particles.[6,7] Although researchers have been able to synthesize CNTs with narrow diameter distribution using narrowly distributed catalyst particles in CVD process, the preparation of catalyst particles with uniform size is not trivial and very time-consuming.[8−13] At the same time, double-walled carbon nanotubes (DWNTs), as the simplest member of the family of multiwalled carbon nanotubes (MWNTs), have attracted attention recently.[14−22] However, the raw materials produced were typically mixtures of DWNTs and single-walled carbon nanotubes (SWNTs), which were also contaminated with catalyst particles and amorphous carbon or even some MWNTs. Recently, Endo et al.[16] reported that more than 95% pure DWNT bundles were synthesized by the methane CVD method with a conditioning catalyst and a two-step purification process. However, controlling the diameter of DWNTs is still a challenge.

In this report, we present a simple CVD method to synthesize DWNTs with narrow diameter distribution. The catalyst used in the experiments was iron disilicide ($FeSi_2$). The as-produced materials showed a DWNT percentage of more than 90% without any purification and a DWNT diameter of 4.5 ± 0.5 nm. We believe such narrow distribution of nanotube diameters arise from the property of the unique catalyst, $FeSi_2$, which has an orthorhombic crystal structure in which the iron and silicon atoms are distributed evenly.[23,24] Such a fact provides the possibility to generate very uniform iron particles on the surface of $FeSi_2$ under appropriate conditions. Another advantage of the catalyst is that $FeSi_2$ is commercially available and can be used as catalyst without any further treatment.

The $FeSi_2$ powder used in our experiment was ordered from Alfa Aesar (CAS no. 12022-99-0) and was loaded on a Si wafer as catalyst. The powder was crushed into smaller pieces by pressing another flat Si wafer on top of the sample. Synthesis of DWNTs was carried out in a 2.5 cm diameter tube furnace. The optimal procedure is described as following: the $FeSi_2$ powders were first heated under 0.5 L/min air flow; after the growth temperature (900 °C) was reached, the samples were heated under an air flow for 20 min; then the system was purged with Ar to remove the air followed by the introduction of carbon feeding gas, which consisted of methane (1500 sccm), ethylene (30 sccm), and H_2 (500 sccm). After a growth time of 10 min, methane and ethylene were turned off and the system was cooled down to room

* Corresponding author. E-mail: j.liu@duke.edu.

10.1021/nl071089a CCC: $37.00
Published on Web 07/26/2007

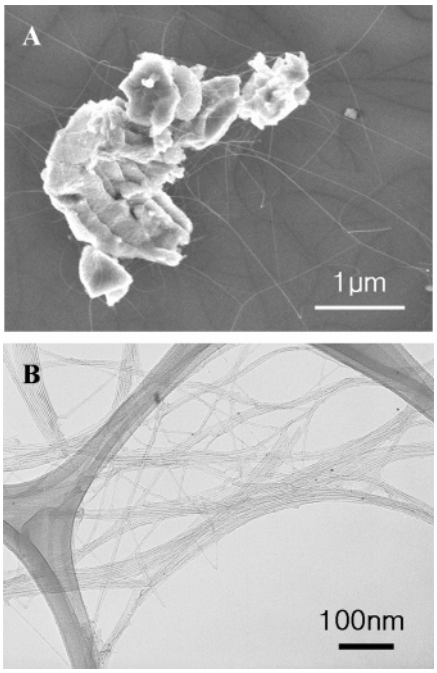

Figure 1. (A) SEM and (B) TEM images of sample prepared with $FeSi_2$ as catalyst.

temperature under the protection of H_2. The nanotubes grown on the catalysts supported on Si wafer were directly imaged with scanning electronic microscopy (SEM). Transmission electronic microscopy (TEM) samples were prepared by sonicating the wafer in ethanol and drop-drying the suspension on TEM grids.

SEM and TEM images of the sample are shown in Figure 1. Representative high-resolution transmission electronic microscopy (HRTEM) images are shown in Figure 2. Examination of many such TEM images revealed that the samples consist mainly of DWNTs, and the average diameter of DWNTs was around 4.5 ± 0.5 nm.

The results showed that $FeSi_2$ can be an effective catalyst for the growth of CNTs. At first, it may look surprising because the formation of $FeSi_2$ was reported to be a negative factor in CNT growth.[25,26] For example, when an Fe film was deposited on Si wafer without SiO_2 coating was used as catalyst, the yield of CNTs were usually very low due to the formation of iron silicide. Thus a buffer layer such as TiN or Si_3N_4 was needed between the Fe film and Si wafer to prevent Fe from reacting with Si.[25,26] However, the major difference between these early experiments, and our approach is the addition of a short oxidation step before the growth of CNTs. X-ray photoelectron spectra (XPS) suggested that such an oxidation step converted the surface of $FeSi_2$ crystals into a thin oxide layer. We believe such an oxide layer is a critical component that provides a route to form stable and uniform catalyst nanoparticles for DWNT growth. In the XPS spectra of the oxidized $FeSi_2$ samples, the peaks at 724.5 and 710.8 eV can be attributed to Fe $2p_{1/2}$ and Fe $2p_{3/2}$ of Fe(III) from Fe_2O_3, respectively, while the peaks in the range of 714−720 and 728−733 eV are the satellite peaks of Fe-(III) (Figure 3A).[27,28] Only one Si peak is shown at 103 eV, which can be attributed to Si(IV) from SiO_2 (Figure 3B).[29,30]

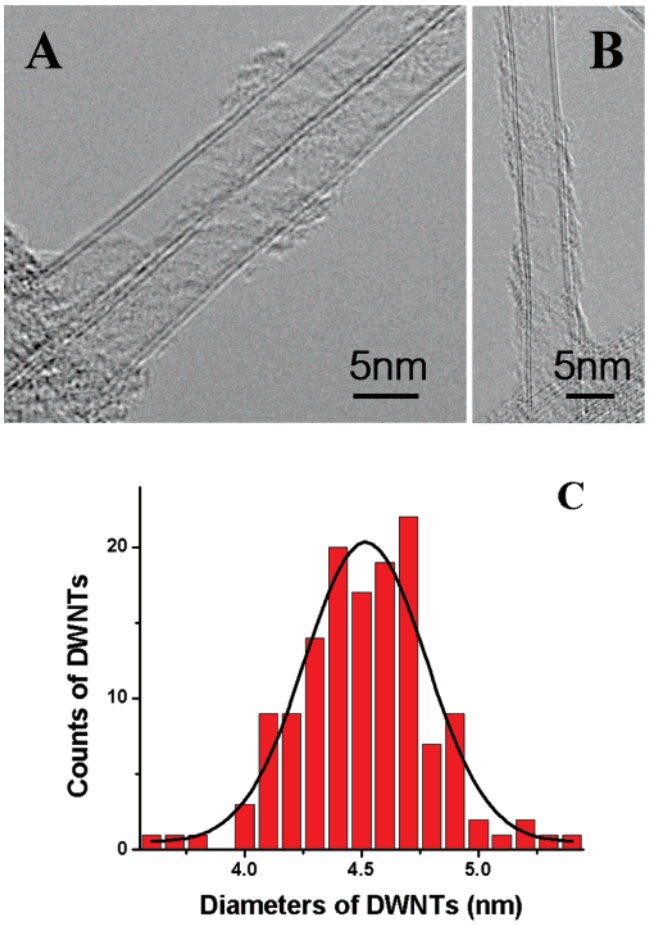

Figure 2. (A and B) HRTEM images of samples prepared with $FeSi_2$ as catalyst and (C) diameter distribution of DWNTs.

To understand the effect of the oxidation step, systematic studies were performed to study the effects of different parameters on the quality of the products. It was found that a proper oxidation of $FeSi_2$ crystal was critical for the growth of uniform DWNT samples. More carbonaceous impurities were obtained when the oxidation time was too long (Figure S1A, Supporting Information). Inhomogeneous distribution of Fe and Si in the oxide layer after a long time oxidation may be responsible for the low purity. There were also more carbonaceous impurities and very low DWNT yield in the samples synthesized without the oxidation step (Figure S1B, Supporting information). XPS spectra show that there are oxide layers on the surface of the $FeSi_2$ crystals even without oxidation at high temperature. However, the oxide layer formed at room temperature is thin and may not be continuous because in the XPS spectra of the sample; other than peaks from Fe(III) and Si(IV), there are also peaks at 719.4, 706.6, and 99 eV. These peaks can be attributed to Fe $2p_{1/2}$, Fe $2p_{3/2}$,[31−33] and Si 2p [29,34] in $FeSi_2$, respectively (Figure 4). XPS spectra also show that on surfaces of $FeSi_2$ crystals without oxidation, the ratio of Si/Fe is 6 and about 75% of Fe is from Fe_2O_3, and the ratio of Si/Fe in oxidized $FeSi_2$ crystals is 60. These results suggest that a low Fe concentration at the $FeSi_2$ surface is important to obtain small but uniform Fe particles. After a proper oxidation step, the $FeSi_2$ crystals were coated with uniform oxide layers and

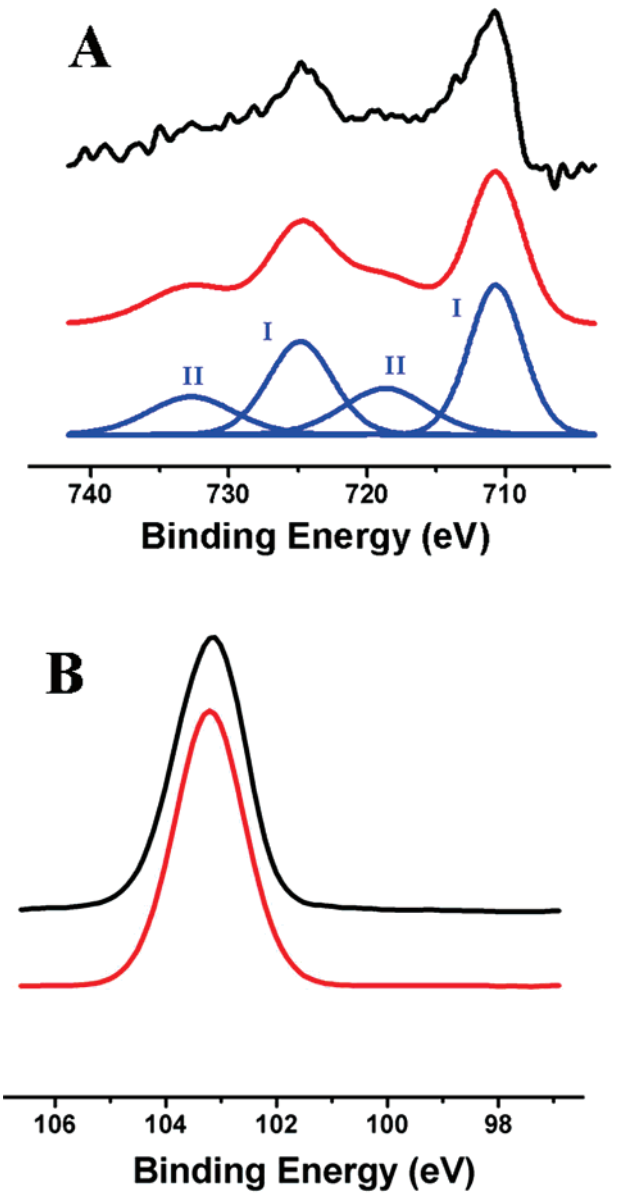

Figure 3. XPS spectra of (A) iron and (B) silicon in $FeSi_2$ after oxidation. The plots from top to bottom are original (black), simulated (red), and splitted spectra (blue) in both (A) and (B). In the splitted spectra of (A), peaks labeled with I, which are at 710.8 and 724.5 eV, are attributed to Fe(III) from Fe_2O_3; peaks labeled with II, which are in the range of 714−720 and 728−733 eV, are satellite peaks of peak I. Only one peak at 103 eV is shown in (B), which suggests all the silicon is Si(IV) in the form of SiO_2.

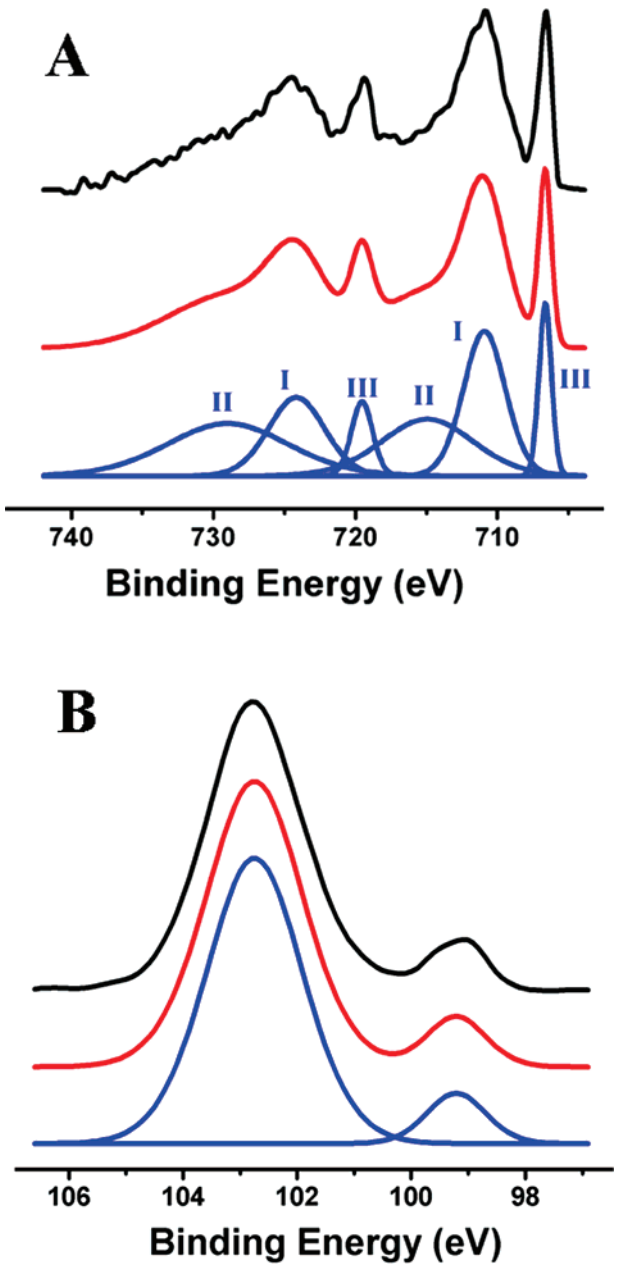

Figure 4. XPS spectra of (A) iron and (B) silicon in $FeSi_2$ without oxidation. The plots from top to bottom are original (black), simulated (red), and splitted spectra (blue) in both (A) and (B). In the splitted spectra of (A), there are new peaks labeled with III, which are at 706.6 and 719.4 eV, are attributed to Fe in $FeSi_2$. Other than the peak at 103 eV, there is one more peak in the splitted spectra of (B), which are at 99 eV and are attributed to Si in $FeSi_2$.

the Fe concentration in oxide layers was also lowered to a proper level. Raman data of the raw CNT samples also confirm the importance of a proper oxidation. The G/D ratio of DWNT samples synthesized from $FeSi_2$ crystals without oxidation was 7.87 while the G/D ratio of DWNT samples from $FeSi_2$ crystals oxidized for 20 min is 12.5 (Figure S2, Supporting Information). The increase of G/D ratio with oxidation suggests that DWNT samples with higher purity were obtained.

Another important step that affects the quality and purity of the as-prepared samples is the reduction of the catalysts before the growth. We have discovered that the best samples were obtained by introducing carbon feeding gas mixed with hydrogen directly after the oxidation step. Addition of a separate reduction process using hydrogen resulted in more carbonaceous impurities, which might be due to the broader distribution of iron particles, as shown in TEM images. This may result from over-reduction of Fe_2O_3 (Figure S3, Supporting Information).

On the basis of these discussions, we outline the growth mechanism of DWNTs with $FeSi_2$ catalysts as follows: first, a homogeneous layer of Fe_2O_3 and SiO_2 mixture is produced on the surface of $FeSi_2$ powders by oxidation, then iron nanoparticles are obtained by the reduction the Fe_2O_3 in the

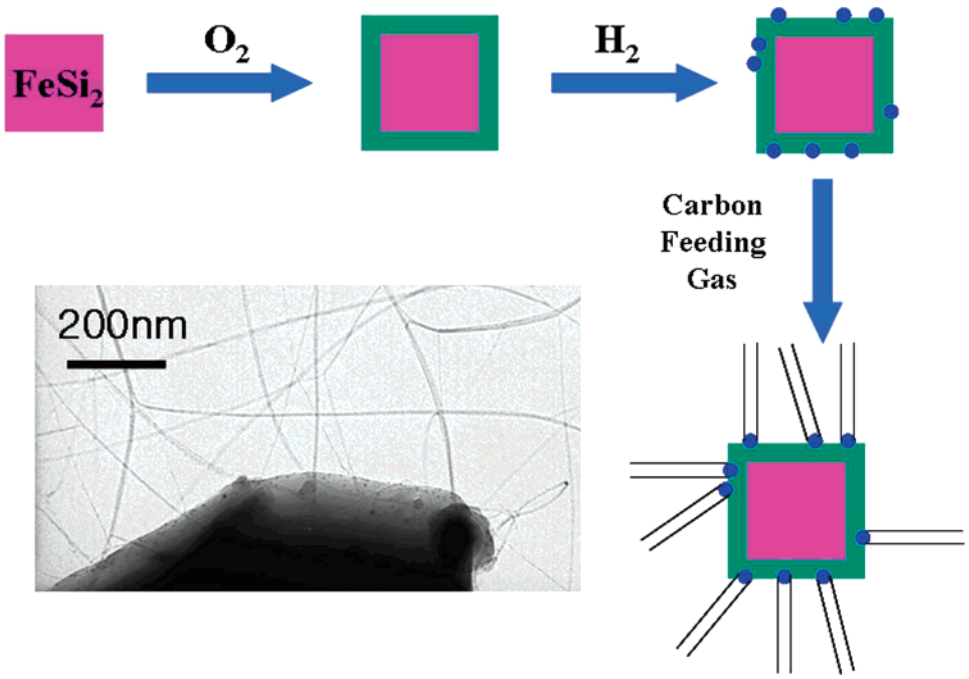

Figure 5. Mechanism of DWNT synthesis with $FeSi_2$ as catalyst.

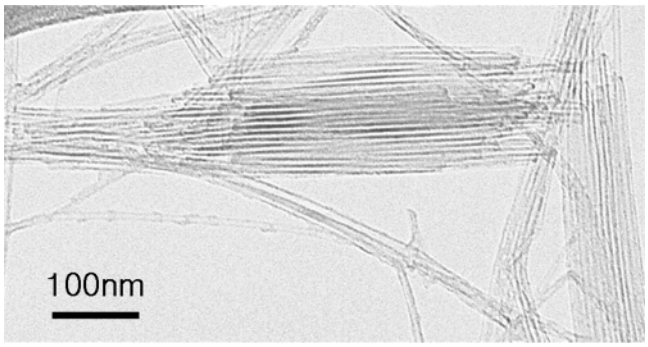

Figure 6. Bundles consisting of short DWNTs with similar length.

oxide layer by the presence of hydrogen, and finally these iron nanoparticles catalyze the growth of DWNTs (Figure 5).

Because the iron and silicon atoms are distributed evenly at atomic scale in $FeSi_2$, uniform iron nanoparticles can be obtained after appropriate oxidation and reduction. In our experiments, only one set of experiment conditions were discovered for the growth of DWNTs with average diameter around 4.5 nm. However, other combinations of the oxidation, reduction, and growth conditions may also exist that will yield other types of nanotubes with uniform diameter and high purity. It is also possible that certain crystalline facets of $FeSi_2$ under our growth conditions produce highly uniform and close-packed catalyst nanoparticles that are suitable for the growth of aligned nanotube bundles. In TEM images of our DWNT samples, it is easy to find small bundles of DWNTs that consist of short DWNTs with similar length (Figure 6 and Figure S4 in Supporting Information) and diameter. Because the overall length distribution of the DWNTs is broad, it is surprising that the DWNTs in such bundles are of similar length. One possible explanation is that these bundles were grown from a closely positioned iron particle array formed on certain lattice facets of $FeSi_2$ and these nanotubes were growing together. If true, the nucleation efficiency of these nanoparticles is much higher than separated nanoparticles. The understanding of such high nucleation efficiency would be important for the development of a CVD process for nanotube production with high yield and good uniformity. More studies are currently underway to optimize the process and study such possibilities.

In summary, we demonstrated that $FeSi_2$, which was previously reported as inactive for nanotube growth, can be used to grow high-purity DWNTs after introducing a proper oxidation step before growth. The DWNTs materials prepared using such a catalyst is not only of high purities but also possess narrow diameter distribution. There are two advantages of using $FeSi_2$ as catalyst compared with other catalysts. One is that uniform iron particles can be easily obtained from $FeSi_2$ through proper oxidation and reduction. The other is that commercial $FeSi_2$ can be employed without any further treatments. More interestingly, the observation of closely packed DWNTs bundles with similar length may prove to be an indication of a catalyst with very high nucleation efficiency. Understanding such a catalyst will enable its use to develop a CVD process for nanotube production with high yield and high uniformity.

Acknowledgment. The work is supported by a grant from DOE (DE-FC36-05GO15103) as part of the Center of Excellence for Carbon-Based Hydrogen Storage. We thank Mr. Tom McNicholas for proofreading during the preparation of the manuscript.

Supporting Information Available: TEM images of sample prepared with a long oxidation of 30 min and without

oxidation; Raman of sample synthesized with a 20 min oxidation step; TEM images of sample prepared with a separate reduction process of 5 and 10 min; bundles consist of short DWNTs with similar length. This material is available free of charge via the Internet at http://pubs.acs.org.

References

(1) Hamada, N.; Sawada, S.-I.; Oshiyama, A. *Phys. Rev. Lett.* **1992**, *68*, 1579.
(2) Saito, R.; Fujita, M.; Dresselhaus, G.; Dresselhaus, M. S. *Appl. Phys. Lett.* **1992**, *60*, 2204.
(3) Cheng, H.; Cooper, A. C.; Pez, G. P.; Kostov, M. K.; Piotrowski, P.; Stuart, S. J. *J. Phys. Chem. B* **2005**, *109*, 3780.
(4) Dillon, A. C.; Jones, K. M.; Bekkedahl, T. A.; Kiang, C. H.; Bethune, D. S.; Heben, M. J. *Nature* **1997**, *386*, 377.
(5) An, L.; Owens, J. M.; McNeil, L. E.; Liu, J. *J. Am. Chem. Soc.* **2002**, *124*, 13688.
(6) Li, Y. M.; Kim, W.; Zhang, Y. G.; Rolandi, M.; Wang, D. W.; Dai, H. J. *J. Phys. Chem. B* **2001**, *105*, 11424.
(7) Cheung, C. L.; Kurtz, A.; Park, H.; Lieber, C. M. *J. Phys. Chem. B* **2002**, *106*, 2429.
(8) Choi, H. C.; Kim, W.; Wang, D. W.; Dai, H. J. *J. Phys. Chem. B* **2002**, *106*, 12361.
(9) Fu, Q.; Huang, S.; Liu, J. *J. Phys. Chem. B* **2004**, *108*, 6124.
(10) Jeong, G.-H.; Yamazaki, A.; Suzuki, S.; Yoshimura, H.; Kobayashi, Y.; Homma, Y. *J. Am. Chem. Soc.* **2005**, *127*, 8238.
(11) Han, S.; Yu, T.; Park, J.; Koo, B.; Joo, J.; Hyeon, T.; Hong, S.; Im, J. *J. Phys. Chem. B* **2004**, *108*, 8091.
(12) Jeong, H. J.; An, K. H.; Lim, S. C.; Park, M.-S.; Chang, J.-S.; Park, S.-E.; Eum, S. J.; Yang, C. W.; Park, C.-Y.; Lee, Y. H. *Chem. Phys. Lett.* **2003**, *380*, 263.
(13) Javey, A.; Dai, H. *J. Am. Chem. Soc.* **2005**, *127*, 11942.
(14) Sugai, T.; Yoshida, H.; Shimada, T.; Okazaki, T.; Shinohara, H.; Bandow, S. *Nano Lett.* **2003**, *3*, 769.
(15) Flahaut, E.; Bacsa, R.; Peigney, A.; Laurent, C. *Chem. Commun.* **2003**, 1442.
(16) Endo, M.; Muramatsu, H.; Hayashi, T.; Kim, Y. A.; Terrones, M.; Dresselhaus, M. S. *Nature* **2005**, *433*, 476.
(17) Hiraoka, T.; Kawakubo, T.; Kimura, J.; Taniguchi, R.; Okamoto, A.; Okazaki, T.; Sugai, T.; Ozeki, Y.; Yoshikawa, M.; Shinohara, H. *Chem. Phys. Lett.* **2003**, *382*, 679.
(18) Ago, H.; Nakamura, K.; Imamura, S.; Tsuji, M. *Chem. Phys. Lett.* **2004**, *391*, 308.
(19) Ramesh, P.; Okazaki, T.; Sugai, T.; Kimura, J.; Kishi, N.; Sato, K.; Ozeki, Y.; Shinohara, H. *Chem. Phys. Lett.* **2006**, *418*, 408.
(20) Hertel, T.; Hagen, A.; Talalaev, V.; Arnold, K.; Hennrich, F.; Kappes, M.; Rosenthal, S.; McBride, J.; Ulbricht, H.; Flahaut, E. *Nano Lett.* **2005**, *5*, 511.
(21) Kalbac, M.; Kavan, L.; Zukalova, M.; Dunsch, L. *Adv. Funct. Mater.* **2005**, *15*, 418.
(22) Kishi, N.; Kikuchi, S.; Ramesh, P.; Sugai, T.; Watanabe, Y.; Shinohara, H. *J. Phys. Chem. B* **2006**, *110*, 24816.
(23) Starke, U.; Weiss, W.; Kutschera, M.; Bandorf, R.; Heinz, K. *J. Appl. Phys.* **2002**, *91*, 6154.
(24) Zheng, Y.; Taccoen, A.; Gandais, M.; Pétroff, J. F. *J. Appl. Cryst.* **1993**, *26*, 388.
(25) de los Arcos, T.; Vonau, F.; Garnier, M. G.; Thommen, V.; Boyen, H.-G.; Oelhafen, P.; Düggelin, M.; Mathis, D.; Guggenheim, R. *Appl. Phys. Lett.* **2002**, *80*, 2383.
(26) Wan, Q.; Wang, T.-H.; Lin, C.-L. *Chin. Phys. Lett.* **2003**, *20*, 301.
(27) Brisk, M. A.; Baker, A. D. *J. Electron Spectrosc. Relat. Phenom.* **1975**, *7*, 197.
(28) Fujimori, A.; Saeki, M.; Kimizuka, N.; Taniguchi, M.; Suga, S. *Phys. Rev. B* **1986**, *34*, 7318.
(29) Klasson, M.; Berndtsson, A.; Hedman, J.; Nilsson, R.; Nyholm, R.; Nordling, C. *J. Electron Spectrosc. Relat. Phenom.* **1974**, *3*, 427.
(30) Barr, T. L.; Lishka, M. A. *J. Am. Chem. Soc.* **1986**, *108*, 3178.
(31) McIntyre, N. S.; Zetaruk, D. G. *Anal. Chem.* **1977**, *49*, 1521.
(32) Asami, K. *J. Electron Spectrosc. Relat. Phenom.* **1976**, *9*, 469.
(33) Lebugle, A.; Axelsson, U.; Nyholm, R.; Martensson, N. *Phys. Scr.* **1981**, *23*, 825.
(34) Hedman, J.; Baer, Y.; Berndtsson, A.; Klasson, M.; Leonhardt, G.; Nilsson, R.; Nordling, C. *J. Electron Spectrosc. Relat. Phenom.* **1972**, *1*, 101.

NL071089A